Large-Strain Dependence of the Acceptor Binding Energy in Germanium

JOHN J. HALL
IBM Watson Laboratory and Columbia University, New York, New York
(Received May 22, 1962)

The strain dependence of the activation energy in p-Ge subject to large ($\sim$0.5%) uniaxial compressional strains has been studied for two different Group III acceptors. For both [100] and [111] compression the energy surfaces have been found to be oblate, that is, $m_\perp > m_{\parallel}$. From Price's theory of the binding-energy strain dependence, the applicable deformation potential elements are found to be $b=-2.1$ eV and $d=-7.0$ eV. Unexpectedly orientation-dependent "chemical shift" effects have been found for both Al and In impurities; the deviation of the binding energy extrapolated to infinite strain from that calculated in the effective-mass approximation is found to be $\sim$4 times as great for [111] strain as for [100] strain. The experimental technique is briefly described.

I. INTRODUCTION

THE study of elastoconductivity phenomena in n-type semiconductors has provided valuable information about the band structure and the donor ground state as well as the various transport properties of both strained and unstrained crystals.[1] In p-type material, however, little information has been published since the initial piezoresistance experiments of Smith[2] and a subsequent paper of Morin, Geballe, and Herring[3]; this is due in large part to the complexity of the valence band which makes accurate interpretation of ordinary piezoresistance effects difficult.[4] Recently, Price[5] has shown that the theory of the strain dependence of the acceptor ground state is quite tractable in the limit of large uniaxial strains and has calculated a provisional value of one of the applicable shear deformation potential elements for germanium from preliminary data of Koenig and Hall.[6] In the present work, additional experimental data will be given for the case treated by Price, and his method will be extended to determine the remaining deformation potential for shear in Ge. Results for different acceptor elements will be compared and the applicability of Price's theory to smaller strain situations will be considered; the behavior of the Hall mobility will also be examined.

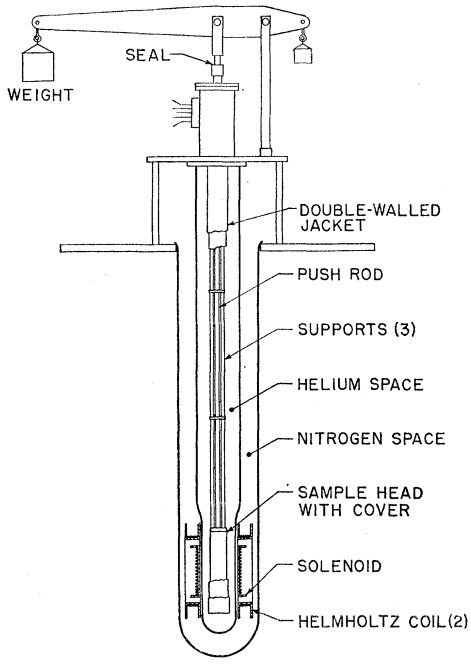

FIG. 1. Apparatus, showing the method of producing the compressive stress to be applied to the sample and the magnet arrangement. A counterweight on the lever arm permits variation of the stress down to zero without removing the push rod from the sample. The resistance heater is located at the bottom of the inner wall of the double-walled jacket.

The effect of a uniaxial strain on the valence band of germanium is to split the normally fourfold degenerate band edge point at $\mathbf{k}=0$ into two doubly degenerate bands separated by an energy E_s,[7–10] which is a linear homogeneous function of the strain amplitude ϵ. Pikus and Bir[8] (PB) have shown that for hole energies $\ll E_s$ (the large-strain limit), the resulting energy surfaces are ellipsoids whose principal axes coincide with those of the strain tensor; in this limit, the effective-mass tensors for the two bands are independent of the strain amplitude and are functions of the strain geometry only.[11]

[1] R. W. Keyes, in *Solid State Physics*, edited by F. Seitz and D. Turnbull (Academic Press Inc., New York, 1960), Vol. 11, p. 149, gives a comprehensive review of the subject and the literature through early 1960.

[2] C. S. Smith, Phys. Rev. **94**, 42 (1954).
[3] Morin, Geballe and Herring, Phys. Rev. **105**, 525 (1957).
[4] G. E. Pikus and G. L. Bir, Soviet Phys.—Solid State **1**, 1675 (1960).
[5] P. J. Price, Phys. Rev. **124**, 713 (1961).
[6] S. H. Koenig and J. J. Hall, Phys. Rev. Letters **5**, 550 (1960).
[7] E. N. Adams, Chicago Midway Laboratories Report CML-TN-P8, 1954 (unpublished).
[8] G. E. Pikus and G. L. Bir, Soviet Phys.—Solid State **1**, 1502 (1960).
[9] W. H. Kleiner and L. M. Roth, Phys. Rev. Letters **2**, 334 (1959).
[10] J. C. Hensel and G. Feher, Phys. Rev. Letters **5**, 307 (1960).
[11] In this discussion we have ignored the $J=\frac{1}{2}$ band split off by the spin orbit interaction. H. Hasegawa (to be published) points out that the effective mass tensor of the $J=3/2$, $M_J=\pm\frac{1}{2}$ band will, in fact, have an explicit strain dependence due to the change in the mixing of this band with the $J=\frac{1}{2}$ band; J. C. Hensel and G. Feher (to be published) have observed this effect

In the notation of PB, E_s may be expressed in terms of two deformation potential elements b and d appropriate to strains of tetragonal and rhombohedral symmetry, respectively, referred to the usual cube axes. A third deformation potential element a describes the equal shift of both bands with dilatation and so does not enter into E_s; this energy contribution shall be ignored in this paper. From the data of reference 3, PB estimate $b \approx 1$ eV and $d \approx 7$ eV, so that to study the transport properties in the approach to the large strain limit at liquid helium temperatures, elastic strains $> 10^{-3}$ must be produced in the samples. Under these conditions essentially all of the holes reside in the upper or thermal band and the strain dependences observed are due to changes in the structure of the thermal band states rather than to repopulation effects between the two bands.

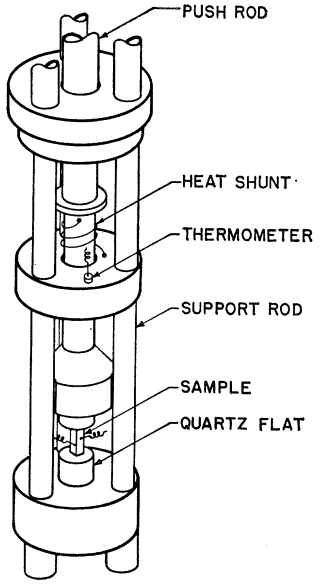

FIG. 2. Detail of the sample head, showing the location of the sample at the point of application of stress. The sample electrical leads are brought out of the head with light-tight feedthroughs, which have been omitted from the figure for clarity.

II. EXPERIMENTAL PROCEDURE

To produce the large strains required, compressive stress is used; the apparatus is shown schematically in Fig. 1. The force to be applied to the sample is produced by a set of weights connected by a 5:1 lever arm to a stainless steel push rod. The latter passes through a sliding vacuum seal to the sample head which is supported from above by three Inconel tubes. The sample head, supports, and push rod are enclosed in a double-walled jacket placed in the helium space of a conventional double Dewar system; a low-pressure exchange gas in the double-walled jacket permits the sample head to be heated above the helium boiling point by a resistance heater (not shown) without excessive helium boiloff. In the liquid nitrogen space a solenoid and a modified Helmholtz pair provide magnetic fields, respectively, parallel and perpendicular to the stress axis for Hall effect measurements. The sample head is shown in Fig. 2 with its light tight cover removed. The sample is placed between two accurately parallel quartz optical flats, the upper connected to the push rod, the lower to the support rods; a carbon resistance thermometer measures the temperature of the enclosure.

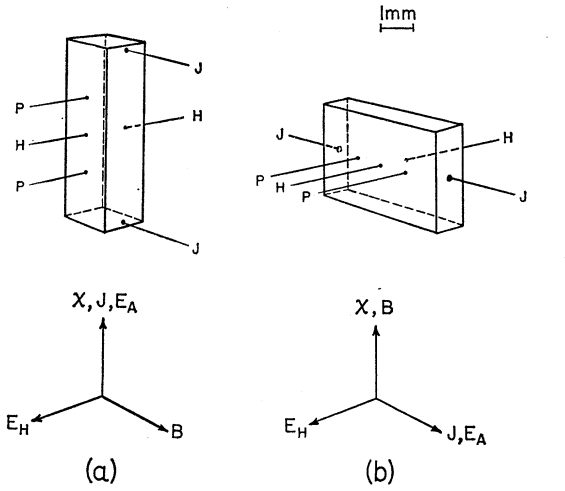

FIG. 3. Sample shape and contact arrangement for measurements (a) with the sample current j parallel to the stress χ and (b) with the current perpendicular to the stress. The pairs of contacts P and H measure the applied voltage and the Hall voltage, respectively, while the current passes through contacts J.

Typical samples are shown to approximate scale in Fig. 3, which also shows the electrical contact arrangements for making four terminal resistivity and Hall effect measurements with the sample current (a) parallel and (b) perpendicular to the stress axis. Ohmic electrical contacts were made by alloying pure tin dots to the samples on a hot stage. The applied voltage, V_A, and the Hall voltage, V_H, were measured independently with two unity gain electrometer followers, whose output difference was fed to one axis of an X-Y recorder, the other axis of which was driven by the output of a feedback electrometer ammeter measuring the sample current. A motor-driven current source permitted continuous plotting of voltage-current characteristics to ensure that low electric field measurements were always made within the region of Ohmic conductivity for p-Ge ($E_A \lesssim 50$ mV/cm). The accuracy of all electrical measurements was $\pm 2\%$ except for the lowest temperature Hall effect for which noise limited accuracy to $\pm 5\%$ in some cases. In addition, small temperature fluctuations in the course of two successive measurements introduced an uncertainty of $\pm 5\%$ in Hall mobility values. The carbon resistance thermometer was calibrated against helium and hydrogen vapor

in cyclotron resonance studies of strained silicon and have used the strain dependence to calculate the deformation potentials. Since the spin-orbit splitting in Ge is an order of magnitude larger than that in Si, the effect in Ge will be proportionately smaller.

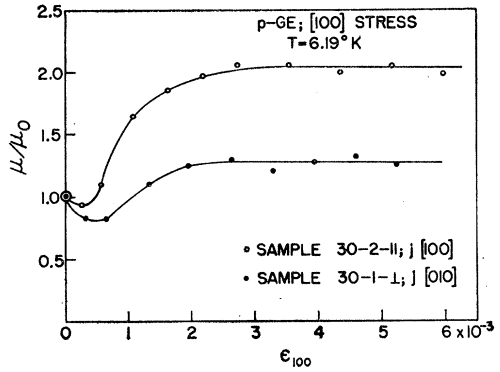

FIG. 4. Hall mobility as a function of strain for current parallel and perpendicular to the [100] stress; $\mu_0=1.5\times10^5$ cm²/V sec.

pressure and was employed over a range for which the estimated accuracy was ±20 mdeg Kelvin.

To ensure uniformity of strain, extreme care in sample preparation was exercised. After x-ray orientation to within 1/10° of arc, the Ge was cut to the desired brick shape and etched; it was then placed in a jig and the faces normal to the stress axis ground and polished optically flat and parallel. In practice, stresses of 8000 kg/cm² can be applied reliably to the samples, irrespective of their crystallographic orientation, without danger of sample failure. For stresses larger than this, failure has occurred in which the sample disintegrates into a fine powder with the abrupt evolution of heat; it has not as yet been determined whether this failure is the result of an intrinsic stress limit of germanium or is due to failure in the apparatus. Strain uniformity was tested by observing the change in the spreading resistance of contacts on opposite sides of the sample; a stress increase of 10% typically produces >100% change in bulk conductivity and hence in the contact resistance and provides a convenient measure of strain uniformity. Strain gradients were also revealed by changes in the electrical symmetry of the Hall contacts caused by shifts in the current flow lines in the sample; this effect was clearly observed in a sample purposely misaligned in the holder and in several early trials in which the sample broke prematurely. None of the samples reported in this work exhibited symptoms of strain nonuniformity; the accuracy of the stress amplitude is limited primarily by the $\pm1\%$ uncertainty in the sample cross section and a residual stress uncertainty of ±10 kg/cm², important only at the very smallest strains.

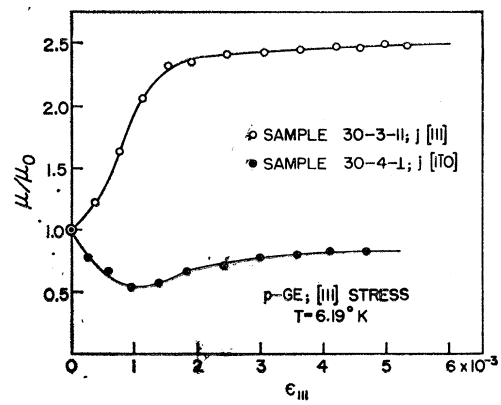

FIG. 5. Hall mobility as a function of strain for current parallel and perpendicular to the [111] stress; $\mu_0=1.5\times10^5$ cm²/V sec.

The samples used in the experiment were cut from two crystals whose characteristics are listed in Table I. The crystals were selected to be reasonably close in major impurity concentration, N_A, and in donor concentration, N_D, and yet to contain group III acceptors differing substantially in activation energy so that the dependence of the data on impurity element could be determined. The acceptor elements listed in Table I are nominal, the measured activation energies being slightly higher than those reported in the literature.[12] The values of N_A-N_D and N_D given were determined from nitrogen and helium temperature Hall-effect measurements and did not vary appreciably for samples cut from different regions of the same crystal.

TABLE I. Characteristics of the crystals from which the samples were prepared.

Crystal No.	Acceptor element	N_A-N_D (cm⁻³)	N_D (cm⁻³)	Activation energy (mV)
30	Al	1.9×10^{14}	$\sim4\times10^{13}$	10.50
71	In	1.5×10^{14}	$\sim2\times10^{13}$	11.52

III. RESULTS

The data are presented in plots of the experimental quantities vs strain or inverse strain, where the strain amplitudes

$$\epsilon_{100}=S_{11}\chi,$$
$$\epsilon_{111}=(S_{11}+2S_{12}+S_{44})\chi/3 \quad (1)$$

have been derived from the experimental stress χ using the elastic compliance constants of Ge at low temperatures determined by Fine.[13] Corrections have been made to all data for dimensional changes which are of the same order of magnitude as the experimental uncertainty.

The variation of the Hall mobility μ with strain is shown in Figs. 4 and 5 for [100] and [111] stress; in both figures, the upper curve corresponds to arrangement (a) of Fig. 3 and the lower curve to arrangement (b). The samples for these data were cut from crystal No. 30 and each had a zero-strain mobility μ_0 of $(1.5\pm0.1)\times10^5$ cm²/V sec at 6.19°K in a magnetic field $B=30$ G. Neither the zero strain mobility nor the

[12] T. H. Geballe and F. J. Morin, Phys. Rev. **95**, 1085 (1954).
[13] M. E. Fine, J. Appl. Phys. **26**, 862 (1955).

ratios of the mobilities for currents (*a*) parallel and (*b*) perpendicular to the stress at large strain showed a clearly interpretable temperature dependence; both quantities decreased approximately 10% from 7 to 5°K, indicating a mixture of neutral and ionized impurity scattering. For this reason, no attempt was made to study the detailed temperature dependence of the mobility. The data do demonstrate conclusively, however, that the Hall mobility for arrangement (*a*) of Fig. 3 is substantially greater than that for arrangement (*b*) for both [100] and [111] compression. For the former case, $(\mu_a/\mu_b)_{100}\approx 1.8$ while for the latter, $(\mu_a/\mu_b)_{111}\approx 2.8$ for the largest strains.

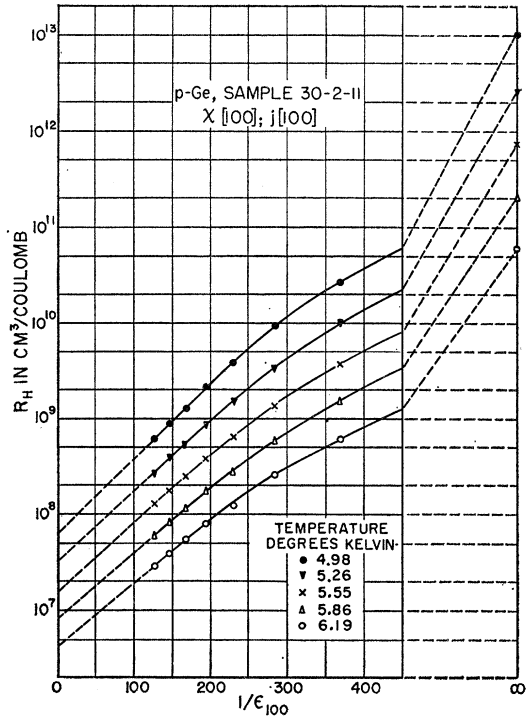

FIG. 6. Hall constant as a function of inverse strain at several temperatures, for current parallel to the [100] stress.

The Hall constant for samples cut from crystal No. 30 is shown in Figs. 6 and 7 for [100] and [111] stress, respectively, as a function of inverse strain $1/\epsilon$; the data were taken at the several temperatures indicated at a field of 30 G. The approach of $\log R_H$ to a linear dependence on $1/\epsilon$ is shown qualitatively by the dashed portions of the curves at small $1/\epsilon$. To permit quantitative analysis of the strain dependence of the acceptor binding energy W, the data of Figs. 6 and 7 and equivalent data for samples cut from crystal No. 71 were reduced to activation energies. For a given value of strain, a value of W was obtained from the slope of $\log(R_H T^{\frac{3}{2}})$ vs $1/T$, thus taking into account the $T^{\frac{3}{2}}$ factor in the density of states for the number of carriers, but ignoring the temperature dependence of the ratio

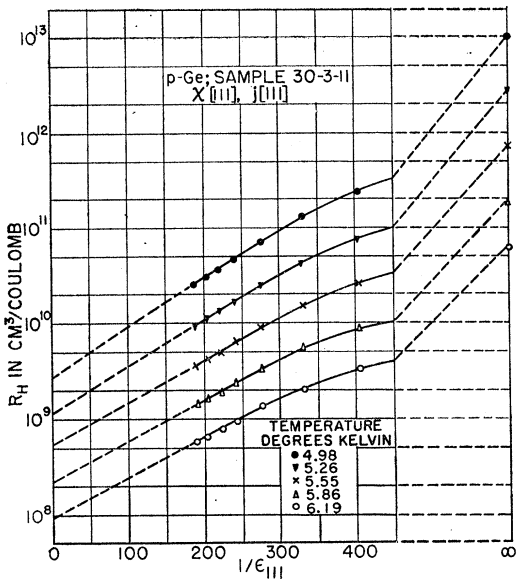

FIG. 7. Hall constant as a function of inverse strain at several temperatures, for current parallel to the [111] stress.

of the drift to Hall mobility; in this manner, the values of $W(\epsilon)$ for [100] and [111] stress, plotted as the experimental points of Figs. 8 and 9, were obtained. As an internal check on the above procedure, the activation energies as functions of strain were recalculated at fixed T, taking for reference the values of W and $\ln R_H$ at the largest strain and assuming $W-W_{\text{ref}}=kT\ln(R_H/R_{H\text{ref}})$; excellent agreement between the two methods was found for $\epsilon>0.2\%$, that is, $1/\epsilon<500$.

The theoretical curves of Figs. 8 and 9 were constructed from the expansion

$$W(\epsilon)=W(\infty)+W_1/\epsilon+W_2/\epsilon^2+\cdots. \qquad (2)$$

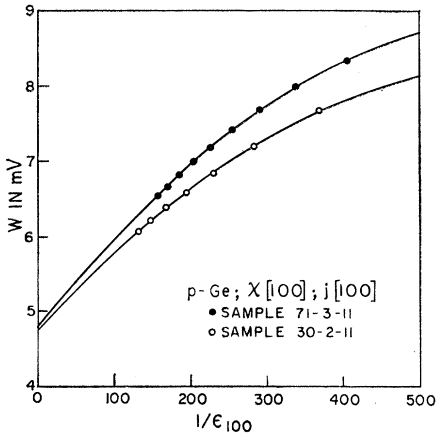

FIG. 8. Activation energy W as a function of inverse strain $1/\epsilon_{100}$ for [100] stress, for samples of Al- and In-doped germanium, Nos. 30 and 71, respectively. The theoretical curves are those calculated from Eq. (2) using the appropriate values of the constants of Table II.

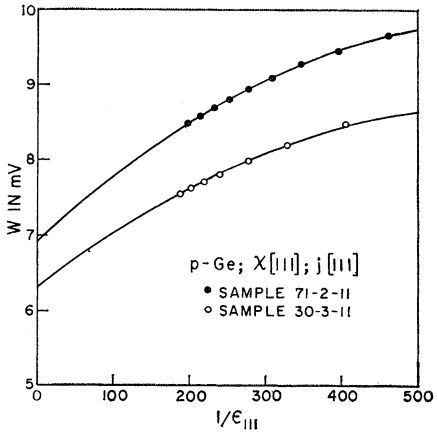

FIG. 9. Activation energy W as a function of inverse strain $1/\epsilon_{111}$ for [111] stress for samples of Al- and In-doped germanium, Nos. 30 and 71, respectively. The theoretical curves are those calculated from Eq. (2) using the appropriate values of the constants of Table II.

The values of the constants were determined by a least squares fit of the data; for values of $1/\epsilon<500$, it was found unnecessary to include terms of order higher than second. Table II lists the values of the constants for the samples of Figs. 8 and 9 which give the best fit, which in all cases is less than 0.01 mV rms deviation. As the data were taken for unequal increments of the argument of (2), the analytic estimation of the uncertainties of the results is refractory. The uncertainties listed with each of the quantities in Table II were determined by varying the input data over the limits of the experimental uncertainty and recalculating the constants, thus giving a range of fit for which the extreme cases are listed. Less extensive data were taken on two additional samples cut from crystal No. 71 to check the reproducibility of the results; the values of the constants for [100] and [111] strains agree closely with the results for samples from the same crystal given in Table II and fall well within the stated uncertainties.

IV. DISCUSSION

In the limit of "infinite" uniaxial strain, that is, infinite energy splitting E_s between the two band edges,[11] the acceptor ground state may be taken as composed solely of Bloch state functions from the nearest lying valence band and may readily be calculated in the effective mass approximation.[14] As E_s is reduced, the ground-state function contains an increasing proportion of states from the band split off by the strain. Price[5] has shown that, if the acceptor binding energy is expanded in terms of the inverse strain amplitude $1/\epsilon$ in the form (2), the term W_1/ϵ determined experimentally above may be equated to the dividend Z_0/E_s, where E_s is proportional to the product of the deformation potential and the strain, and Z_0 is a quantity

[14] W. Kohn and J. M. Luttinger, Phys. Rev. **98**, 915 (1955).

TABLE II. Results of a least-squares fit of the data of Figs. 8 and 9 to Eq. (2) up to second order in $1/\epsilon$.

Crystal No. and acceptor	Stress direction	$W(\infty)$ (mV)	W_1 (10^{-3}mV)	W_2 (10^{-6}mV)
30 (Al)	[100]	4.75±0.15	11.2±1.5	−8.8±3.0
	[111]	6.30±0.25	8.0±2.0	−6.7±2.7
71 (In)	[100]	4.78±0.15	13.0±1.5	−10.2±2.5
	[111]	6.76±0.15	9.4±1.6	−7.5±2.4

calculable for the infinite strain ground state in the effective mass approximation.

To obtain Z_0, Price[5] expands the dispersion relation for the valence band, given by Eq. (14) of PB, from the large strain limit to first order in $1/E_s$:

$$E(\epsilon,\mathbf{k})=\begin{cases}+\frac{1}{2}E_s+H_+(\mathbf{k})+Z(\mathbf{k})/E_s\\ -\frac{1}{2}E_s+H_-(\mathbf{k})-Z(\mathbf{k})/E_s,\end{cases} \tag{3}$$

where $H_\pm(\mathbf{k})$ are simple ellipsoidal energy functions of $\mathbf{k}$ appropriate to the upper and the lower of the split bands. Depending upon the sign of E_s, that is, the sign of the product of the deformation potential and the strain, either of the energy functions (3) may correspond to that of the thermal band. In the effective mass approximation,[14] the infinite strain binding energy $W(\infty)$ is the ground state of the operator $H(-i\nabla)+U(\mathbf{r})$, where $U(\mathbf{r})$ is the acceptor ion potential. If the wave function of the infinite strain ground state is expanded,

$$\psi_0(\mathbf{r})=\sum_{\mathbf{k}} a_{\mathbf{k}}\varphi_{\mathbf{k}}(\mathbf{r}), \tag{4}$$

in terms of the Bloch states of the thermal band edge, then

$$Z_0=\sum_{\mathbf{k}}|a_{\mathbf{k}}|^2 Z(\mathbf{k}), \tag{5}$$

or, in terms of the envelope wave function $\Psi_0(\mathbf{r})$,

$$Z_0=\int \Psi_0 Z(-i\nabla)\Psi_0 d^3\mathbf{r}. \tag{6}$$

For example, consider a [111] uniaxial compression with strain components

$$\epsilon_{xx}=-\epsilon_{111},\quad \epsilon_{yy}=\epsilon_{zz}=r'\epsilon_{111},\quad \epsilon_{xy}=\cdots=0, \tag{7}$$

where $r'=-(S_{11}+2S_{12}-\frac{1}{2}S_{44})/(S_{11}+2S_{12}+S_{44})$ is the Poisson ratio for this strain. In the coordinate system [111], [01$\bar{1}$], [$\bar{2}$11], expansion of Eq. (14) of PB in the form (3) yields

$$E_s=-2d(1+r')\epsilon_{111}/\sqrt{3}, \tag{8}$$

$$H_\pm(\mathbf{k})=(A\pm D/\sqrt{3})k_x^2+(A\mp D/2\sqrt{3})(k_y^2+k_z^2), \tag{9}$$

and

$$Z(\mathbf{k})=(2B^2+D^2/3)k_x^2(k_y^2+k_z^2)+(B^2/4+D^2/6)(k_y^2+k_z^2)^2, \tag{10}$$

TABLE III. Derived quantities for [100] and [111] compressional stress assuming $m_\perp > m_{||}$ for these cases.

Stress orientation	$m_\perp/m_{||}$	$a_{||}$ (Å)	$a_\perp$ (Å)	$W(\infty)$ (mV)	Z_0 (mV²)
[100]	2.45	129	93	4.29	63.6
[111]	3.18	130	86	4.50	80.1

where A, B and $D \equiv N/\sqrt{3}$ are the inverse cyclotron mass constants.[15] In (10) several small cross terms odd in k_y or k_z which do not contribute to Z_0 have been omitted; Z_0 may now be calculated from (6) with the usual approximation for the ground-state envelope function[14]

$$\Psi_0 = (\pi a_\perp^2 a_{||})^{-\frac{1}{2}} \exp\left[-\left(\frac{x^2}{a_{||}^2}+\frac{y^2+z^2}{a_\perp^2}\right)^{\frac{1}{2}}\right], \quad (11)$$

yielding

$$Z_0 = \frac{2B^2}{3}\left(\frac{1}{a_\perp^4}+\frac{2}{a_{||}^2 a_\perp^2}\right)+\frac{2D^2}{9}\left(\frac{2}{a_\perp^4}+\frac{1}{a_{||}^2 a_\perp^2}\right). \quad (12)$$

Price[5] has obtained the equivalent result for a [100] compressional strain

$$\epsilon_{xx} = -\epsilon_{100}, \quad \epsilon_{yy} = \epsilon_{zz} = r\epsilon_{100}, \quad \epsilon_{xy} = \cdots = 0, \quad (13)$$

where $r = -S_{12}/S_{11}$. Referred to electron state energies, his Eqs. (12), (13), and (16) become

$$E_s = -2b(1+r)\epsilon_{100}, \quad (14)$$

$$H_\pm(\mathbf{k}) = (A \pm B)k_x^2 + (A \mp \tfrac{1}{2}B)(k_y^2+k_z^2), \quad (15)$$

and

$$Z_0 = \frac{B^2}{a_\perp^4}+\frac{D^2}{3}\left(\frac{1}{a_\perp^4}+\frac{2}{a_{||}^2 a_\perp^2}\right). \quad (16)$$

The energy functions (9) and (15) permit the determination of the parameters $a_\perp$ and $a_{||}$ of (11), (12), and (16) from the inverse cyclotron mass constants once the anisotropy of the thermal band is known. The Hall mobility data of Figs. 4 and 5 show that for both [100] and [111] compressional stress, the mobility for current parallel to the stress is greater than that for current perpendicular to the stress. If we assume the anisotropy of the scattering to be small, we may conclude that in the thermal band $m_\perp > m_{||}$ for both strain orientations (cf. the tentative conclusion of reference 6); this result is in agreement with recent cyclotron resonance measurements on strained Ge.[16] The variational calculation of Keyes[17] for this case provides $a_\perp$ and $a_{||}$ as well as $W(\infty)$ for [100] and [111] compression; Table III lists the results derived for these quantities and Z_0 using the values of the inverse cyclotron mass parameters of Frankl and Levinger,[18] $A = -13.27$, $|B| = 8.63$, and $|D| = 19.42$. The dielectric constant $\varkappa$ was taken to be 16.0.

TABLE IV. Results for the deformation potentials b and d and the infinite strain chemical shift $\Delta_c(\infty)$ for differently doped crystals and [100] and [111] compression from Eqs. (17), (18), and (19).

Stress orientation	Deformation potential, V		$\Delta_c(\infty)$, mV	
	No. 30 (Al)	No. 71 (In)	No. 30 (Al)	No. 71 (In)
[100]	$b = -2.2 \pm 0.2$	$b = -1.9 \pm 0.2$	0.46 ± 0.15	0.49 ± 0.15
[111]	$d = -7.5 \pm 1.8$	$d = -6.4 \pm 1.1$	1.80 ± 0.20	2.26 ± 0.15

From Tables II and III the values of the deformation potential elements b and d may be derived using the relations

$$b = -Z_0/2(1+r)W_1 \quad (17)$$

for [100] compression and

$$d = -\sqrt{3}Z_0/2(1+r')W_1 \quad (18)$$

for [111] compression, obtained from (14) and (8), respectively, by equating Z_0/E_s with the experimentally determined W_1/ϵ. Table IV lists the values obtained using $r = 0.272$ and $r' = 0.154$ from the data of Fine.[13] The experiments determine only the algebraic sign of the products bB or dD, which may be seen from (3) by reversing the signs of both d and D in (8) and (9) or b and B in (14) and (15); experimentally, both products are positive. The signs given with b and d in Table IV were obtained assuming the parameters B and D to be negative.[19,20] Recently, Il'ina and Kurova[21] concluded from their experiments on p Ge subject to [110] uniaxial compression that the dD product is negative, in conflict with the conclusions of this paper and the more direct evidence of cyclotron resonance.[16] Their conclusion, if correct, would modify the results given here considerably; however, at the present time the weight of the evidence favors the opposite case.[22]

Table IV also presents values of the infinite strain "chemical shift" effect,[14]

$$\Delta_c(\infty) \equiv W(\infty)_{\text{exp}} - W(\infty)_{\text{calc}}, \quad (19)$$

[15] G. Dresselhaus, A. F. Kip and C. Kittel, Phys. Rev. **98**, 368 (1955).

[16] T. R. Loree, M. H. Halloran and R. N. Dexter, Bull. Am. Phys. Soc. **6**, 426 (1961); R. N. Dexter (private communication); J. C. Hensel (private communication). Professor Dexter also informed the author that the anisotropy of the relaxation time, measured from the resonance linewidth, was not significant. The result $m_\perp > m_{||}$ was previously reported by the author [Bull. Am. Phys. Soc. **6**, 426 (1961)], in which the word "prolate" was inadvertently used for "oblate."

[17] R. W. Keyes, IBM J. Research Develop. **5**, 65 (1961).

[18] B. W. Levinger and D. R. Frankl, J. Phys. Chem. Solids **20**, 281 (1961).

[19] E. O. Kane, J. Phys. Chem. Solids **1**, 82 (1956).

[20] W. Kohn, in *Solid State Physics*, edited by F. Seitz and D. Turnbull (Academic Press Inc., New York, 1957), Vol. 5, p. 257.

[21] M. A. Il'ina and I. A. Kurova, Soviet Phys.—JETP **14**, 61 (1962).

[22] In reference 6, the dD product was also tentatively identified as negative; however, it has subsequently been verified that the two-terminal measurements of the conductivity normal to the stress were misinterpreted because of the very large changes in the contact resistance under strain.

TABLE V. Empirical determination of Z_0 and the deformation potential elements b and d from the data of Table II using Eqs. (23) and (24). $W(0)$ is the zero-strain binding energy calculated from (25).

Crystal No. and acceptor	Stress direction	Deformation potential (V)	Z_0 (mV²)	$W(0)$ (mV)
30 (Al)	[100]	$b=-2.4\pm0.4$	70±20	11.1±1.5
	[111]	$d=-5.7\pm1.5$	60±25	11.7±2.0
71 (In)	[100]	$b=-2.4\pm0.3$	80±15	11.7±1.2
	[111]	$d=-6.4\pm1.2$	80±25	12.0±1.8

taken from Tables II and III for both dopants and orientations. The chemical shift is a measure of the failure of the effective mass approximation (and the associated variational calculations) to describe the impurity ion ground state; its origin presumably lies in effects arising in the immediate neighborhood of the impurity ion.[2] The accuracy of the values of Z_0 calculated in the effective mass approximation in Table III, and of the values of the constants b and d in Table IV, depends upon the fractional smallness of $\Delta_c(\infty)$ compared to $W(\infty)$.[5] For [100] oriented crystals, $\Delta_c(\infty)$ is only $\sim 10\%$ of $W(\infty)$ and not significantly dependent upon the dopant, whereas for the [111] case, $\Delta_c(\infty)$ is large, as much as 50% for crystal No. 71, and differs substantially for the two acceptor elements. For this reason, the values of b in Table IV are considered somewhat more reliable than those of d; noting that the values of b and d do not differ by more than the experimental uncertainty between the two dopants, the final values for the deformation potential elements determined by this experiment are

$$b=-2.1\pm0.2 \text{ eV}; \quad d=-7.0\pm1.5 \text{ eV}. \tag{20}$$

In his discussion of the acceptor binding energy, Price[5] suggests the expression

$$W=W(\infty)+Z_0/(E_s+W), \tag{21}$$

as an approximation at smaller strains. Equation (21) does not entail neglecting the chemical shift effects, the condition for its validity presumably being that $W-W(\infty)$ be small compared to $W(\infty)$; this condition is reasonably well satisfied for the data of Figs. 8 and 9. Expanding (21) in the form (2) to second order in $1/E_s$, one obtains

$$W=W(\infty)+Z_0/E_s-W(\infty)Z_0/E_s^2. \tag{22}$$

Z_0 and E_s may now be determined in terms of the experimental quantities W_1 and W_2 of Table II by equating (2) and (22) term by term:

$$E_s/\epsilon=-W(\infty)W_1/W_2 \tag{23}$$

and

$$Z_0=-W(\infty)W_1^2/W_2; \tag{24}$$

the appropriate deformation potential elements are then given by (8) and (14). Table V gives the results of this procedure for the data of Table II; the last column of Table V lists the zero-strain value of the binding energy, $W(0)$, obtained by setting $E_s=0$ in (21), yielding Eq. (21) of reference 5:

$$W(0)=\tfrac{1}{2}\{W(\infty)+[W(\infty)^2+4Z_0]^{\frac{1}{2}}\}. \tag{25}$$

It is clear from Table V that (22) agrees with the more restricted results of Table IV well within the (generous) experimental uncertainties. Equation (21) in its most extreme application, that for zero strain, is also in good agreement with experiment (Table I). One may therefore conclude that (21) is a good approximation of the strain dependence of the binding energy in the limits (22) and (25). A more challenging test of (21) would be to fit the activation energy over the entire range of available stress; unfortunately, the substantial changes expected in the ratio of the Hall to the drift mobility at small strains would obscure the strain dependence of the binding energy in this region.

The values of Z_0 in Table V do not differ greatly from those calculated in the effective mass approximation in Table III; however, the values of Table V show closer agreement for different orientations of the same crystal than for different crystals with the same strain orientation. This suggests that chemical shift effects in Z_0, though not so important as for the binding energy, are more important than orientation effects. This is certainly not the case for the infinite strain binding energy; here, there seems to be little difference between dopants when compared to the striking orientation dependence of $\Delta_c(\infty)$. Part of the large shift for the [111] samples may be only apparent due to small errors in the cyclotron mass parameters, to which the calculated values of $W(\infty)$ and Z_0 are both quite sensitive. In addition, one expects that the central core corrections to the infinite strain ground-state wave function will be more important to the extent to which the wave function density is greater in the neighborhood of the ion core;[20,23] since the ground-state envelope is more prolate for [111] than for [100] infinite strain, the resultant shift should be slightly greater for the former. At the present time, however, neither of these corrections seems adequate to explain the observations.

V. CONCLUSION

The study of the large-strain dependence of the acceptor binding energy has provided more reliable values of the deformation potential elements for the valence band than ordinary piezoresistance experiments because of the greater tractability of the theory. Knowledge of these deformation potentials permits, for example, the calculation of the hole lattice mobility in the unstrained crystal.[24] In addition, new and unex-

[23] K. Narita and T. Shimizu, J. Phys. Soc. Japan **16**, 2588 (1961).

[24] M. Tiersten, Bull Am. Phys. Soc. **7**, 77 (1962), and (to be published).

pected chemical shift effects become manifest in the approach to infinite strain. The utility of the large strain technique described here extends to the study of other transport properties as well: With the availability of purer material, one may study the strain and temperature dependence of the lattice mobility at or near the large strain limit.[25] Finally, it will be of interest to compare the deformation potentials now being determined for Ge by cyclotron resonance studies of strained material[26] with those obtained here in the effective-mass approximation.

[25] P. J. Price and Yi-Han Kao, IBM J. Research Develop. **5**, 63 (1961).
[26] J. C. Hensel (private communication).

ACKNOWLEDGMENTS

I wish to thank S. H. Koenig, with whom this work was initiated, for his encouragement. P. J. Price's stimulating arguments and continuing interest in the work were indispensable. In addition, I thank R. D. Brown III and Miss A. Willner for experimental and computational assistance, Mrs. C. Pfister for the x-ray orientations, and the many other members of the Watson Laboratory staff who were of invaluable assistance. J. C. Hensel and R. N. Dexter kindly informed me of their results before publication. The crystals used in the experiments were provided by T. H. Geballe of the Bell Telephone Laboratories and M. Ranaldi of the IBM Components Division.

PHYSICAL REVIEW VOLUME 128, NUMBER 1 OCTOBER 1, 1962

Theory of Double Magnetic Resonance in Solids

B. N. PROVOTOROV
Institute of Chemical Physics, Academy of Sciences, Moscow, U. S. S. R.
(Received April 27, 1962)

Expressions accounting for the changes in the shape of absorption lines for solids under conditions of double magnetic resonance were obtained. The shift of the absorption line maximum for one of the resonance frequencies with increase of saturation of the other resonance frequency was calculated. The expressions obtained are in agreement with experiment.

THE behavior of aluminum samples under conditions of double magnetic resonance was investigated in a recently published work carried out by Holcomb, Pederson, and Sliker.[1] The authors succeeded in observing a number of interesting properties displayed in the saturation of the sample by one of the radio-frequency fields.

The present note is concerned with the theoretical treatment of double resonance under conditions of magnetic-resonance saturation with respect to one frequency.

The frequencies and amplitudes of the rf fields will be denoted by ν_1, ν_2 and H_1, H_2, respectively. One of the rf fields will be assumed weak compared with the other: $H_2 \ll H_1$.

Let us begin by considering the most simple case, $H_1 \ll H_{\text{loc}}$. (Here $H_{\text{loc}}=\mu/d^3$, where μ is the magnetic moment of an individual particle and d is the separation between neighboring magnetic particles.) Due to the smallness of H_2 its value may be taken, to a first approximation, as zero. The problem will then be restricted to that of saturation for ordinary magnetic resonance. This was discussed by the author in a previous paper,[2] which contained the following expressions for the stationary values of the full spin projection on the direction of the constant magnetic field $I_z(t)$ and for the average energy of the spin-spin interaction $H_{ss}^0(t)$:

$$I_{z\,\text{st}}=I_{z0}\frac{1+\gamma^2H_1^2\times\frac{1}{2}g(\nu_1)T_1h^2(\Delta\nu_1)^2/2H_0^2}{1+\gamma^2H_1^2\times\frac{1}{2}g(\nu_1)T_1[1+h^2(\Delta\nu_1)^2/2H_0^2]}, \quad (1)$$

$$\frac{h\Delta\nu_1(H_{ss}^0)_{\text{st}}}{H_0^2}=I_{z0}\frac{\gamma^2H_1^2\times\frac{1}{2}g(\nu_1)T_1h^2(\Delta\nu_1)^2/2H_0^2}{1+\gamma^2H_1^2\times\frac{1}{2}g(\nu_1)T_1[1+h^2(\Delta\nu_1)^2/2H_0^2]}. \quad (2)$$

Here $\Delta\nu_1=\nu_1-\nu_0$, $\nu_0=\gamma H_0/2\pi$, T_1 is the spin-lattice relaxation time $I_z(t)$, $g(\nu)$ is a function normalized to unity and describing the absorption line shape in the absence of saturation,

$$H_0^2=\text{Spur}(H_{ss}^0)^2/\text{Spur}I_z^2,$$

I_z is the operator of full spin projection on the direction of the constant magnetic field, and H_{ss}^0 is the operator of the secular part of the spin-spin interaction.

In accordance with reference 2, the energy of the H_2 field absorbed by the spin system per unit time is

$$P(\nu_2,H_2)=h\nu_2\gamma^2H_2^2\times\tfrac{1}{2}g(\nu_2)\times(I_{z\,\text{st}}-h\Delta\nu_2(H_{ss}^0)_{\text{st}}/H_0^2). \quad (3)$$

Here $\Delta\nu_2=\nu_2-\nu_0$.

[1] D. F. Holcomb, B. Pedersen, and T. Sliker, Phys. Rev. **123**, 1951 (1961).
[2] B. N. Provotorov, J. Exptl. Theoret. Phys. (U.S.S.R.) **41**, 1582 (1961) [translation: Soviet Phys.—JETP **5**, 1126 (1962)].